# ASSESSING THE INFLUENCE OF UNCERTAIN PARAMETERS ON THE VIBRATION QUALITY OF CARS

## NGHIÊN CỨU KHẢO SÁT ẢNH HƯỞNG CỦA CÁC THÔNG SỐ KẾT CẤU ĐẾN DAO ĐỘNG CỦA Ô TÔ CON

**Nguyen Ngoc Tram**[1], **Kieu Duc Thinh**[1,*], **Vu Van Tan**[2], **Olivier Sename**[3]

DOI: http://doi.org/10.57001/huih5804.2025.128

**ABSTRACT**

During the operation of a car, structural parameters such as vehicle body mass, damping coefficient of the shock absorber, tire stiffness, vehicle speed, and other parameters are continuously changing. These parameters directly affect the car's vibrations. This study focuses on the uncertainty of three key parameters: vehicle body mass, damping coefficient of the shock absorber, and suspension stiffness. A general model of car with 7 degrees of freedom is developed to evaluate ride comfort and road safety. The impact of these uncertain structural parameters on the system's characteristics is assessed by varying the values between 50 - 150% of the initial values in the time and frequency domains using Matlab's "ureal" function. The simulation results in both domains under different conditions showed that the uncertain parameters significantly affect the car's ride comfort and road safety.

***Keywords:*** *Vehicle dynamics, motion safety, ride comfort, uncertain parameters, suspension system.*

**TÓM TẮT**

Trong quá trình hoạt động của ô tô, các thông số kết cấu như khối lượng thân xe, hệ số cản của giảm chấn, độ cứng của lốp, vận tốc di chuyển của ô tô, và một số thông số khác là đại lượng thay đổi liên tục, do vậy những thông số này ảnh hưởng trực tiếp đến dao động của ô tô. Nghiên cứu này trình bày đến tính không chắc chắn của ba thông số chính: khối lượng thân xe, hệ số cản của giảm chấn, độ cứng của lốp. Trước tiên mô hình tổng quát ô tô con với 7 bậc tự do đã được xây dựng để đánh giá độ êm dịu và an toàn chuyển động. Để đánh giá mức độ ảnh hưởng của các thông số kết cấu đến đặc tính hệ thống, các thông số không chắc chắn nêu trên được khảo sát trong khoảng 50 - 150% giá trị ban đầu trên miền thời gian và miền tần số thông qua chức năng ureal của phần mềm Matlab. Kết quả mô phỏng trên miền thời gian và miền tần số ở các chế độ khác nhau đã cho thấy các thông số không chắc chắn khảo sát có ảnh hưởng rất lớn đến độ êm dịu và an toàn chuyển động của ô tô.

***Từ khóa:*** *Động lực học ô tô, độ an toàn chuyển động, độ êm dịu chuyển động, thông số không chắc chắn, hệ thống treo ô tô.*

[1]Faculty of Mechanical Engineering, Thuyloi University, Vietnam
[2]Faculty of Mechanical Engineering, University of Transport and Communications, Vietnam
[3]University Grenoble Alpes, CNRS, Grenoble INP, GIPSA-Lab, Grenoble, France
[*]Email: kieuducthinh@tlu.edu.vn
Received: 22/12/2024
Revised: 13/2/2025
Accepted: 28/5/2025

### 1. INTRODUCTION

In recent years, car vibrations have become a key research topic. The main cause of car vibrations comes from road surface excitations. The suspension system is used to moderate these vibrations, aiming to enhance ride comfort and safety. The suspension system divides the car into two parts: the sprung mass (all parts above the suspension) and the unsprung mass (all parts below the suspension). The suspension system consists of two main components: the elastic element and the damper.

The suspension system plays a crucial role in directly affecting the smoothness of the ride, ensuring the

transmission of forces from the wheels, guiding ability, and the workspace of the suspension system, especially when the car moves on rough roads. Vehicle motion safety is mainly limited by the vertical displacement of the wheels, the roll of the sprung mass during braking, or cornering. Ride comfort can be evaluated by vertical displacement, vertical acceleration, and the pitching motion of the sprung mass.

Many studies have examined car vibrations using models such as ¼, ½, and full car models. The ¼ car model [1-8], the ½ car model [9-11], and the full car model [12-14] have been studied for car dynamics and vibrations. However, most research stops at evaluating the uncertainty of parameters for ¼ and ½ models, and there are very few studies on full car models. For instance, Semiha Turkay and Huseyin Akcay [2] used the ¼ car model to evaluate ride comfort during lateral and longitudinal movements. W Gao, N Zhang, J C Ji, and H P Du [3] studied the vibrations of the ¼ car model considering parameter uncertainties, including sprung and unsprung masses, damping coefficient, and stiffness of the spring and tire.

In this paper, a full car model with 7 degrees of freedom is simulated to evaluate motion safety and comfort, considering uncertainties in structural parameters like body mass, damping coefficient, and suspension stiffness. These values are varied from 50% to 150% of their original values to assess the system's vibrations. Time-domain and frequency-domain simulations is conducted, showing the influence of these uncertain parameters on the vehicle's ride comfort and road safety.

The paper is structured into five sections as follows: Section 2 presents the development of a general car vibration model. Section 3 outlines the criteria for selecting uncertain parameters. Section 4 presents simulation results and evaluations in both the time and frequency domains. The conclusion of the paper is provided in Section 5

## 2. MATHEMATICAL MODEL FORMULATION

The model studied is a general full car vibration model with 7 degrees of freedom: vertical displacement of the car body (Z); pitch and roll angles (φ, θ); and vertical displacement at the four wheels ($Z_1$, $Z_2$, $Z_3$, $Z_4$). The general model is shown in Figure 1, and the parameters of the model are summarized in Table 1 [15].

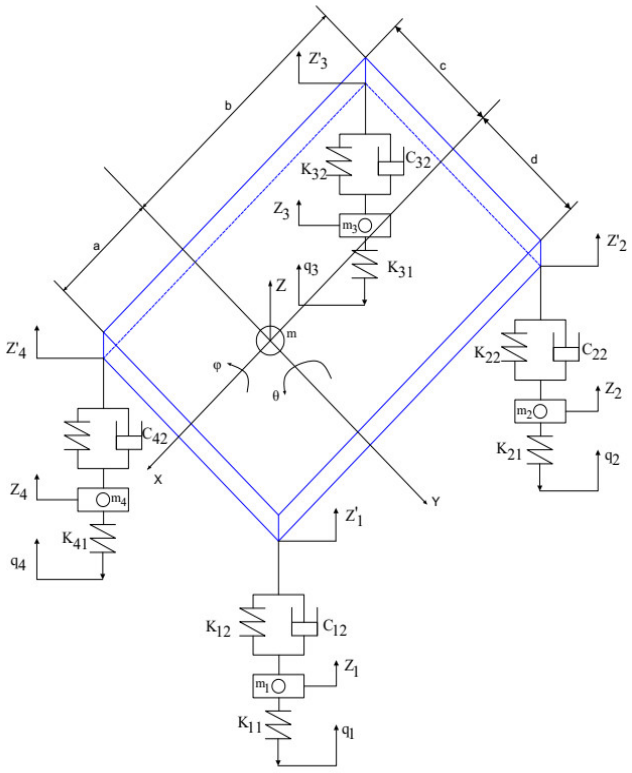


Figure 1. A Full Car Vibration Model

Table 1. Parameters of full car model [22]

| STT | Parameters | Symbol | Values | Unit |
|---|---|---|---|---|
| 1 | Unsprung mass of wheels 1 and 4 | $m_1$, $m_4$ | 30.2 | kg |
| 2 | Unsprung mass of wheels 2 and 3 | $m_2$,$m_3$ | 49.7 | kg |
| 3 | Body mass | m | 1150 | kg |
| 4 | Tire stiffness | $k_{11}$, $k_{21}$, $k_{31}$, $k_{41}$ | 181000 | N/m |
| 5 | Suspension stiffness (each wheel) | $k_{12}$, $k_{22}$, $k_{32}$, $k_{42}$ | 30000 | N/m |
| 6 | Damping coefficient | $c_1$, $c_2$, $c_3$, $c_4$ | 1400 | N.s/m |
| 7 | Moment of inertia about Y-axis | $J_Y$ | 861.8 | kg.m$^2$ |
| 8 | Moment of inertia about X-axis | $J_X$ | 330,5 | kg.m$^2$ |
| 9 | Distance from center of gravity to front axle | a | 1.116 | m |
| 10 | Distance from center of gravity to rear axle | b | 1.232 | m |
| 11 | Distance from center of gravity to left track | d | 0.621 | m |
| 12 | Distance from center of gravity to right track | c | 0.621 | m |
| 13 | Vehicle speed | V | | km/h |

The dynamic equations of the car are established based on the principle of separating individual subsystems and D'Alembert's principle, as follows:

$$
\begin{cases}
m.\ddot{Z} = Z.\left(-K_{12}-K_{22}-K_{32}-K_{42}\right)+\dot{Z}.\left(-C_{12}-C_{22}-C_{32}-C_{42}\right)+\varphi.\left(-d.K_{12}+c.K_{22}-d.K_{32}+c.K_{42}\right)+\dot{\varphi}.\left(-d.C_{12}+c.C_{22}-d.C_{32}+c.C_{42}\right)\\
\quad+\theta.\left(a.K_{12}+a.K_{22}-b.K_{32}-b.K_{42}\right)+\dot{\theta}.\left(a.C_{12}+a.C_{22}-b.C_{32}-b.C_{42}\right)+Z_1.\left(K_{12}\right)\\
\quad+\dot{Z}_1.\left(C_{12}\right)+Z_2.\left(K_{22}\right)+\dot{Z}_2.\left(C_{22}\right)+Z_3.\left(K_{32}\right)+\dot{Z}_3\left(C_{32}\right)+Z_4.\left(K_{42}\right)+\dot{Z}_4\left(C_{42}\right);\\
J_x.\ddot{\varphi} = Z.\left(-d.K_{12}-d.K_{32}+c.K_{42}+c.K_{42}\right)+\dot{Z}.\left(-d.C_{12}-d.C_{32}+c.C_{42}+c.C_{22}\right)+\varphi.\left(-d^2.K_{12}-d^2.K_{32}-c^2.K_{42}-c^2.K_{22}\right)\\
\quad+\dot{\varphi}.\left(-d^2.C_{12}-d^2.C_{32}-c^2.C_{42}-c^2.C_{22}\right)+\theta.\left(a.d.K_{12}-b.d.K_{32}+b.c.K_{42}.\theta-a.c.K_{22}\right)+\dot{\theta}.\left(a.d.C_{12}-b.d.C_{32}+b.c.C_{42}-a.c.C_{22}\right)\\
\quad+Z_1.\left(d.K_{12}\right)+\dot{Z}_1.\left(d.C_{12}\right)+Z_2.\left(-c.K_{22}\right)+\dot{Z}_2.\left(-c.C_{22}\right)+Z_3.\left(d.K_{32}\right)+\dot{Z}_3\left(d.C_{32}\right)+Z_4.\left(-c.K_{42}\right)+\dot{Z}_4\left(-c.C_{42}\right);\\
J_y.\ddot{\theta} = Z.\left(a.K_{12}-b.K_{32}-b.K_{42}+a.K_{22}\right)+\dot{Z}.\left(a.C_{12}-b.C_{32}-b.C_{42}+a.C_{22}\right)+\varphi.\left(a.d.K_{12}-b.d.K_{32}+b.c.K_{42}-a.c.K_{22}\right)\\
\quad+\dot{\varphi}.\left(a.d.C_{12}-b.d.C_{32}+b.c.C_{42}-a.c.C_{22}\right)+\theta.\left(-a^2.K_{12}-b^2.K_{32}-b^2.K_{42}-a^2.K_{22}\right)\\
\quad+\dot{\theta}.\left(-a^2.C_{12}-b^2.C_{32}-b^2.C_{22}-a^2.C_{22}\right)+Z_1.\left(-a.K_{12}\right)+\dot{Z}_1.\left(-a.C_{12}\right)+Z_2.\left(-a.K_{22}\right)+\dot{Z}_2.\left(-a.C_{22}\right)\\
\quad+Z_3.\left(b.K_{32}\right)+\dot{Z}_3.\left(b.C_{32}\right)+Z_4.\left(b.K_{42}\right)+\dot{Z}_4.\left(b.C_{42}\right);\\
m_1.\ddot{Z}_1 = Z.\left(K_{12}\right)+\dot{Z}.\left(C_{12}\right)+\varphi.\left(d.K_{12}\right)+\dot{\varphi}.\left(d.C_{12}\right)+\theta.\left(-a.K_{12}\right)+\dot{\theta}.\left(-a.C_{12}\right)+Z_1.\left(-K_{11}-K_{12}\right)+\dot{Z}_1.\left(-C_{12}\right)+K_{11}.q_1;\\
m_2.\ddot{Z}_2 = Z.\left(K_{22}\right)+\dot{Z}.\left(C_{22}\right)+\varphi.\left(-c.K_{22}\right)+\dot{\varphi}\left(-c.C_{22}\right)+\theta.\left(-a.K_{22}\right)+\dot{\theta}.\left(-a.C_{22}\right)+Z_2.\left(-K_{22}-K_{21}\right)+\dot{Z}_2.\left(-C_{22}\right)+K_{21}.q_2;\\
m_3.\ddot{Z}_3 = Z.\left(K_{32}\right)+\dot{Z}.\left(C_{32}\right)+\varphi.\left(d.K_{32}\right)+\dot{\varphi}.\left(d.C_{32}\right)+\theta.\left(b.K_{32}\right)+\dot{\theta}.\left(b.C_{32}\right)+Z_3.\left(-K_{31}-K_{32}\right)+\dot{Z}_3.\left(-C_{32}\right)+K_{31}.q_3;\\
m_4.\ddot{Z}_4 = Z.\left(K_{42}\right)+\dot{Z}.\left(C_{42}\right)+\varphi.\left(-c.K_{42}\right)+\dot{\varphi}.\left(-c.C_{42}\right)+\theta.\left(b.K_{42}\right)+\dot{\theta}.\left(b.C_{42}\right)+Z_4.\left(-K_{41}-K_{42}\right)+\dot{Z}_4.\left(-C_{42}\right)+K_{41}.q_4;
\end{cases}
\tag{1}
$$

Equation (1) is written in the following form:

$$
\begin{cases}
\ddot{Z}=\dfrac{\left(-K_{12}-K_{22}-K_{32}-K_{42}\right)}{m}Z+\dfrac{\left(-C_{12}-C_{22}-C_{32}-C_{42}\right)}{m}\dot{Z}+\dfrac{\left(-d.C_{12}-d.C_{22}+c.C_{32}+c.C_{42}\right)}{m}\varphi+\dfrac{\left(-d.C_{12}+c.C_{22}-d.C_{32}+c.C_{42}\right)}{m}\dot{\varphi}\\
\quad+\dfrac{\left(a.K_{12}+a.K_{22}-b.K_{32}-b.K_{42}\right)}{m}\theta+\dfrac{\left(a.C_{12}+a.C_{22}-b.C_{32}-b.C_{42}\right)}{m}\dot{\theta}\\
\quad+\dfrac{\left(K_{12}\right)}{m}Z_1+\dfrac{\left(C_{12}\right)}{m}\dot{Z}_1+\dfrac{\left(K_{22}\right)}{m}Z_2+\dfrac{\left(C_{22}\right)}{m}\dot{Z}_2+\dfrac{\left(K_{32}\right)}{m}Z_3+\dfrac{\left(C_{32}\right)}{m}\dot{Z}_3+\dfrac{\left(K_{42}\right)}{m}Z_4+\dfrac{\left(C_{42}\right)}{m}\dot{Z}_4;\\
\ddot{\varphi}=\dfrac{\left(-d.K_{12}-d.K_{32}+c.K_{42}+c.K_{42}\right)}{J_x}Z+\dfrac{\left(-d.C_{12}-d.C_{32}+c.C_{42}+c.C_{22}\right)}{J_x}\dot{Z}+\dfrac{\left(-d^2.K_{12}-d^2.K_{32}-c^2.K_{42}-c^2.K_{22}\right)}{J_x}\varphi\\
\quad+\dfrac{\left(-d^2.C_{12}-d^2.C_{32}-c^2.C_{42}-c^2.C_{22}\right)}{J_x}\dot{\varphi}+\dfrac{\left(a.d.K_{12}-b.d.K_{32}+b.c.K_{42}.\theta-a.c.K_{22}\right)}{J_x}\theta+\dfrac{\left(a.d.C_{12}-b.d.C_{32}+b.c.C_{42}-a.c.C_{22}\right)}{J_x}\dot{\theta}\\
\quad+\dfrac{\left(d.K_{12}\right)}{J_x}Z_1+\dfrac{\left(d.C_{12}\right)}{J_x}\dot{Z}_1+\dfrac{\left(-c.K_{22}\right)}{J_x}Z_2+\dfrac{\left(-c.C_{22}\right)}{J_x}\dot{Z}_2+\dfrac{\left(d.K_{32}\right)}{J_x}Z_3+\dfrac{\left(d.C_{32}\right)}{J_x}\dot{Z}_3+\dfrac{\left(-c.K_{42}\right)}{J_x}Z_4+\dfrac{\left(-c.C_{42}\right)}{J_x}\dot{Z}_4;\\
\ddot{\theta}=\dfrac{\left(a.K_{12}-b.K_{32}-b.K_{42}+a.K_{22}\right)}{J_y}Z+\dfrac{\left(a.C_{12}-b.C_{32}-b.C_{42}+a.C_{22}\right)}{J_y}\dot{Z}+\dfrac{\left(a.d.K_{12}-b.d.K_{32}+b.c.K_{42}-a.c.K_{22}\right)}{J_y}\varphi\\
\quad+\dfrac{\left(a.d.C_{12}-b.d.C_{32}+b.c.C_{42}-a.c.C_{22}\right)}{J_y}\dot{\varphi}+\dfrac{\left(-a^2.K_{12}-b^2.K_{32}-b^2.K_{42}-a^2.K_{22}\right)}{J_y}\theta+\dfrac{\left(-a^2.C_{12}-b^2.C_{32}-b^2.C_{22}-a^2.C_{22}\right)}{J_y}\dot{\theta}\\
\quad+\dfrac{\left(-a.K_{12}\right)}{J_y}Z_1+\dfrac{\left(-a.C_{12}\right)}{J_y}\dot{Z}_1+\dfrac{\left(-a.K_{12}\right)}{J_y}Z_2+\dfrac{\left(-aK_{22}\right)}{J_y}\dot{Z}_2+\dfrac{\left(b.K_{32}\right)}{J_y}Z_3+\dfrac{\left(b.C_{32}\right)}{J_y}\dot{Z}_3+\dfrac{\left(b.K_{42}\right)}{J_y}Z_4+\dfrac{\left(b.C_{42}\right)}{J_y}\dot{Z}_4;\\
\ddot{Z}_1=\dfrac{\left(K_{12}\right)}{m_1}Z+\dfrac{\left(C_{12}\right)}{m_1}\dot{Z}+\dfrac{\left(d.K_{12}\right)}{m_1}\varphi+\dfrac{\left(d.C_{12}\right)}{m_1}\dot{\varphi}+\dfrac{\left(-a.K_{12}\right)}{m_1}\theta+\dfrac{\left(-a.C_{12}\right)}{m_1}\dot{\theta}+\dfrac{\left(-K_{11}-K_{12}\right)}{m_1}Z_1+\dfrac{\left(-C_{12}\right)}{m_1}\dot{Z}_1+\dfrac{K_{11}.q_1}{m_1};\\
\ddot{Z}_2=\dfrac{\left(K_{22}\right)}{m_2}Z+\dfrac{\left(C_{22}\right)}{m_2}\dot{Z}+\dfrac{\left(-c.K_{22}\right)}{m_2}\varphi+\dfrac{\left(-c.C_{22}\right)}{m_2}\dot{\varphi}+\dfrac{\left(-a.K_{22}\right)}{m_2}\theta+\dfrac{\left(-a.C_{22}\right)}{m_2}\dot{\theta}+\dfrac{\left(-K_{22}-K_{21}\right)}{m_2}Z_2+\dfrac{\left(-C_{22}\right)}{m_2}\dot{Z}_2+\dfrac{K_{21}.q_2}{m_2};\\
\ddot{Z}_3=\dfrac{\left(K_{32}\right)}{m_3}Z+\dfrac{\left(C_{32}\right)}{m_3}\dot{Z}+\dfrac{\left(d.K_{32}\right)}{m_3}\varphi+\dfrac{\left(d.C_{32}\right)}{m_3}\dot{\varphi}+\dfrac{\left(b.K_{32}\right)}{m_3}\theta+\dfrac{\left(b.C_{32}\right)}{m_3}\dot{\theta}+\dfrac{\left(-K_{31}-K_{32}\right)}{m_3}Z_3+\dfrac{\left(-C_{32}\right)}{m_3}\dot{Z}_3+\dfrac{K_{31}.q_3}{m_3};\\
\ddot{Z}_4=\dfrac{\left(K_{42}\right)}{m_4}Z+\dfrac{\left(C_{42}\right)}{m_4}\dot{Z}+\dfrac{\left(-c.K_{42}\right)}{m_4}\varphi+\dfrac{\left(-c.C_{42}\right)}{m_4}\dot{\varphi}+\dfrac{\left(b.K_{42}\right)}{m_4}\theta+\dfrac{\left(b.C_{42}\right)}{m_4}\dot{\theta}+\dfrac{\left(-K_{41}-K_{42}\right)}{m_4}Z_4+\dfrac{\left(-C_{42}\right)}{m_4}\dot{Z}_4+\dfrac{K_{41}.q_4}{m_4};
\end{cases}
\tag{2}
$$

The equation is rewritten in the state-space representation as follows:

$$
\begin{cases}
X = AX+BU\\
Y = CX+DU
\end{cases}
\tag{3}
$$

Where the state vector is:

$X=[Z, \dot{Z}, \varphi, \dot{\varphi}, \theta, \dot{\theta}, Z_1, \dot{Z}_1, Z_2, \dot{Z}_2, Z_3, \dot{Z}_3, Z_4, \dot{Z}_4]$.

The output vector is:

$Y=[Z, \dot{Z}, \varphi, \dot{\varphi}, \theta, \dot{\theta}, Z_1, \dot{Z}_1, Z_2, \dot{Z}_2, Z_3, \dot{Z}_3, Z_4, \dot{Z}_4, \ddot{Z}, \ddot{\varphi}, \ddot{\theta}]$.

The disturbance vector is the road profile u=[$q_1, q_2, q_3, q_4$]. The matrices A, B, C, and D are defined as follows:

$$B = \begin{bmatrix} B_{7x4} \\ B_{10x4} \end{bmatrix}; \quad B_{7x4} = \text{zero}(7x4);$$

$$A = \begin{bmatrix} A_{6x6} & A_{6x8} \\ A_{8x6} & A_{8x8} \end{bmatrix}; \; A_{6x6} = \begin{bmatrix} a_1 & a_2 \end{bmatrix}$$

$$a_1 = \begin{bmatrix} 0 & 1 & 0 \\ \frac{-K_{12}-K_{22}-K_{32}-K_{42}}{m} & \frac{-C_{12}-C_{22}-C_{32}-C_{42}}{m} & \frac{-d.K_{12}-c.K_{22}-d.K_{32}+c.C_{42}}{m} \\ 0 & 0 & 0 \\ \frac{-d.K_{12}+c.K_{22}-d.K_{32}+c.K_{42}}{J_x} & \frac{-d.C_{12}+c.C_{22}-d.C_{32}+c.C_{42}}{J_x} & \frac{-d^2.K_{12}-c^2.K_{22}-d^2.K_{32}-c^2.K_{42}}{J_x} \\ 0 & 0 & 0 \\ \frac{a.K_{12}+a.K_{22}-b.K_{32}-b.K_{42}}{J_y} & \frac{a.C_{12}+a.C_{22}-b.C_{32}-b.C_{42}}{J_y} & \frac{a.d.K_{12}-a.c.K_{22}-b.d.K_{32}+b.c.K_{42}}{J_y} \end{bmatrix};$$

$$a_2 = \begin{bmatrix} 0 & 0 & 0 \\ \frac{-d.C_{12}+c.C_{22}-d.C_{32}+c.C_{42}}{m} & \frac{a.K_{12}+a.K_{22}-b.K_{32}-b.K_{42}}{m} & \frac{a.C_{12}+a.C_{22}-b.C_{32}-b.C_{42}}{m} \\ 1 & 0 & 0 \\ \frac{-d^2.C_{12}-c^2.C_{22}-d^2.C_{32}-c^2.C_{42}}{J_x} & \frac{a.d.K_{12}-a.c.K_{22}-b.d.K_{32}-b.c.K_{42}}{J_x} & \frac{a.d.C_{12}-a.c..C_{22}-b.d.C_{32}+b.c.C_{42}}{J_x} \\ 0 & 0 & 0 \\ \frac{a.d.C_{12}-a.c.C_{22}-b.d.C_{32}+b.c.C_{42}}{J_y} & \frac{-a^2.K_{12}-a^2.K_{22}-b^2.K_{32}-b^2.K_{42}}{J_y} & \frac{-a^2.C_{12}-a^2.C_{22}-b^2.C_{32}-b^2.C_{42}}{J_y} \end{bmatrix};$$

$$A_{6x8} = \begin{bmatrix} 0 & 0 & 0 & 0 & 0 & 0 & 0 & 0 \\ \frac{K_{12}}{m} & \frac{C_{12}}{m} & \frac{K_{22}}{m} & \frac{C_{22}}{m} & \frac{K_{32}}{m} & \frac{C_{32}}{m} & \frac{K_{42}}{m} & \frac{C_{42}}{m} \\ 0 & 0 & 0 & 0 & 0 & 0 & 0 & 0 \\ \frac{d.K_{12}}{J_x} & \frac{d.C_{12}}{J_x} & \frac{-c.K_{22}}{J_x} & \frac{-c.C_{22}}{J_x} & \frac{d.K_{32}}{J_x} & \frac{d.C_{32}}{J_x} & \frac{-c.K_{42}}{J_x} & \frac{-c.C_{42}}{J_x} \\ 0 & 0 & 0 & 0 & 0 & 0 & 0 & 0 \\ \frac{-a.K_{12}}{J_y} & \frac{-a.C_{12}}{J_y} & \frac{-a.K_{22}}{J_y} & \frac{-a.C_{22}}{J_y} & \frac{K_{32}}{J_y} & \frac{b.C_{32}}{J_y} & \frac{b.K_{42}}{J_y} & \frac{b.C_{42}}{J_y} \end{bmatrix}$$

$$A_{8x8} = \begin{bmatrix} 0 & 1 & 0 & 0 & 0 & 0 & 0 & 0 \\ \frac{-K_{11}-K_{12}}{m_1} & \frac{-C_{12}}{m_1} & 0 & 0 & 0 & 0 & 0 & 0 \\ 0 & 0 & 0 & 1 & 0 & 0 & 0 & 0 \\ 0 & 0 & \frac{-K_{21}-K_{22}}{m_2} & \frac{-C_{22}}{m_2} & 0 & 0 & 0 & 0 \\ 0 & 0 & 0 & 0 & 0 & 1 & 0 & 0 \\ 0 & 0 & 0 & 0 & \frac{-K_{31}-K_{32}}{m_3} & \frac{C_{32}}{m_3} & 0 & 0 \\ 0 & 0 & 0 & 0 & 0 & 0 & 0 & 1 \\ 0 & 0 & 0 & 0 & 0 & 0 & \frac{-K_{41}-K_{42}}{m_4} & \frac{-C_{42}}{m_4} \end{bmatrix}$$

$$B_{10\times4}=\begin{bmatrix} \frac{K_{11}}{m_1} & 0 & 0 & 0 \\ 0 & 0 & 0 & 0 \\ 0 & \frac{K_{21}}{m_2} & 0 & 0 \\ 0 & 0 & 0 & 0 \\ 0 & 0 & \frac{K_{31}}{m_3} & 0 \\ 0 & 0 & 0 & 0 \\ 0 & 0 & 0 & \frac{K_{41}}{m_4} \end{bmatrix}$$

$$C=\begin{bmatrix} C_1 & C_2 & C_3 \\ C_4 & C_5 & C_6 \end{bmatrix};$$

$$C_1=\begin{bmatrix} 1&0&0\\0&1&0\\0&0&1\\0&0&0\\0&0&0\\0&0&0\\0&0&0\\0&0&0\\0&0&0\\0&0&0\\0&0&0\\0&0&0\\0&0&0\\0&0&0 \end{bmatrix};\ C_2=\begin{bmatrix} 0&0&0\\0&0&0\\0&0&0\\1&0&0\\0&1&0\\0&0&1\\0&0&0\\0&0&0\\0&0&0\\0&0&0\\0&0&0\\0&0&0\\0&0&0\\0&0&0 \end{bmatrix};\ C_3=\begin{bmatrix} 0&0&0&0&0&0&0&0\\0&0&0&0&0&0&0&0\\0&0&0&0&0&0&0&0\\0&0&0&0&0&0&0&0\\0&0&0&0&0&0&0&0\\0&0&0&0&0&0&0&0\\1&0&0&0&0&0&0&0\\0&1&0&0&0&0&0&0\\0&0&1&0&0&0&0&0\\0&0&0&1&0&0&0&0\\0&0&0&0&1&0&0&0\\0&0&0&0&0&1&0&0\\0&0&0&0&0&0&1&0\\0&0&0&0&0&0&0&1 \end{bmatrix};$$

$$C_4=\begin{bmatrix} \frac{(-K_{12}-K_{22}-K_{32}-K_{42})}{m} & \frac{(-C_{12}-C_{22}-C_{32}-C_{42})}{m} & \frac{-d.K_{12}-c.K_{22}-d.K_{32}+c.C_{42}}{m} \\ \frac{-d.K_{12}+c.K_{22}-d.K_{32}+c.K_{42}}{J_x} & \frac{-d.C_{12}+c.C_{22}-d.C_{32}+c.C_{42}}{J_x} & \frac{-d^2.K_{12}-c^2.K_{22}-d^2.K_{32}-c^2.K_{42}}{J_x} \\ \frac{a.K_{12}+a.K_{22}-b.K_{32}-b.K_{42}}{J_y} & \frac{a.C_{12}+a.C_{22}-b.C_{32}-b.C_{42}}{J_y} & \frac{a.d.K_{12}-a.c.K_{22}-b.d.K_{32}+b.c.K_{42}}{J_y} \end{bmatrix};$$

$$C_5=\begin{bmatrix} \frac{(-d.C_{12}+c.C_{22}-d.C_{32}+c.C_{42})}{m} & \frac{(a.K_{12}+a.K_{22}-b.K_{32}-b.K_{42})}{m} & \frac{(a.C_{12}+a.C_{22}-b.C_{32}-b.C_{42})}{m} \\ \frac{-d^2.C_{12}-c^2.C_{22}-d^2.C_{32}-c^2.C_{42}}{J_x} & \frac{a.d.K_{12}-a.c.K_{22}-b.d.K_{32}-b.c.K_{42}}{J_x} & \frac{a.d.C_{12}-a.c..C_{22}-b.d.C_{32}+b.c.C_{42}}{J_x} \\ \frac{a.d.C_{12}-a.c.C_{22}-b.d.C_{32}+b.c.C_{42}}{J_y} & \frac{-a^2.K_{12}-a^2.K_{22}-b^2.K_{32}-b^2.K_{42}}{J_y} & \frac{-a^2.C_{12}-a^2.C_{22}-b^2.C_{32}-b^2.C_{42})}{J_y} \end{bmatrix};$$

$$C_6=\begin{bmatrix} \frac{K_{12}}{m} & \frac{C_{12}}{m} & \frac{K_{22}}{m} & \frac{C_{22}}{m} & \frac{K_{32}}{m} & \frac{C_{32}}{m} & \frac{K_{42}}{m} & \frac{C_{42}}{m} \\ \frac{d.K_{12}}{J_x} & \frac{d.C_{12}}{J_x} & \frac{-c.K_{22}}{J_x} & \frac{-c.C_{22}}{J_x} & \frac{d.K_{32}}{J_x} & \frac{d.C_{32}}{J_x} & \frac{-c.K_{42}}{J_x} & \frac{-c.C_{42}}{J_x} \\ \frac{-a.K_{12}}{J_y} & \frac{-a.C_{12}}{J_y} & \frac{-a.K_{22}}{J_y} & \frac{-a.C_{22}}{J_y} & \frac{K_{32}}{J_y} & \frac{b.C_{32}}{J_y} & \frac{b.K_{42}}{J_y} & \frac{b.C_{42}}{J_y} \end{bmatrix};$$

D = zero(17,4);

## 3. UNCERTAINTY PARAMETERS IN THE MODEL

The uncertainty of parameters and the uncertainty of the model are particularly important to consider when building probabilistic risk assessments. In many optimization and decision-making problems, uncertainty about parameters can be modeled and addressed through methods such as optimization under uncertainty, decision theory, and planning methods in uncertain environments.

For automotive suspension systems, uncertainty includes parameters such as the vehicle's speed, sprung mass, unsprung mass, damping coefficient, tire stiffness, and actuator mechanisms. Uncertainty in hydraulic-electrical actuators has been shown to significantly affect the characteristics and performance of actuators in active suspension systems. In the referenced paper [17], an LPV controller was used, where the author monitored parameters and planned appropriately within the LPV control framework. This controller was designed to ensure the desired performance and stability requirements of the closed-loop system. By automatically adjusting suspension system parameters such as damping force and spring stiffness, these systems enhance oscillation amplitude and meet the required comfort and safety standards [18-21]. In passenger car suspension systems, parameter uncertainty refers to the fact that the values of system model parameters are not precisely known. Therefore, parameter uncertainty can lead to issues in the control system, such as reduced performance, instability, and decreased durability [8].

In MATLAB software, the author uses Uncertain Real Parameter (ureal) to analyze model parameters. An uncertain real parameter is characterized by a nominal value, stored in the NominalValue property, and an associated uncertainty, which represents the potential deviation from this nominal value. The

ureal object encodes this uncertainty in three distinct ways: PlusMinus (Represents uncertainty as an absolute deviation added to or subtracted from the nominal value); Range (Defines uncertainty as an absolute range of possible values, independent of the nominal value); Percentage (Quantifies uncertainty as a percentage deviation from the nominal value). In the context of this research, the authors utilized the "Percentage" mode in MATLAB. This mode quantifies uncertainty as a percentage deviation from the nominal value. In this study, with a nominal value of 100 and an uncertainty of ±50%, the parameter value can range from 50% to 150%.

In this study, the author chooses the vehicle body mass, damping coefficient, and suspension stiffness as uncertain parameters for investigation. The focus is on examining the characteristics of parameter uncertainty in the structural parameters of cars to assess parameter uncertainty and vehicle instability during operation. This is because, during vehicle operation, the body mass continuously changes from unloaded to fully loaded, and may even exceed the load. Two values for the damping coefficient C and suspension stiffness K are selected with fixed values in Table 1; however, during operation, these two parameters are nonlinear variables and only fluctuate around their equilibrium positions.

## 4. SIMULATION AND EVALUATION OF RESULTS

### 4.1. Survey Conditions

The authors investigated the vehicle's vibrations in both time and frequency domains based on two criteria: ride comfort and road safety. In the frequency domain, they examined the amplitude of the transfer function of the wheel across a range from 0 to 100 rad/s. In the time domain, the authors analyzed the vehicle's vibrations while driving on a sinusoidal road profile with an excitation frequency of ω = 20 rad/s. In this section, the characteristics of the uncertain structural parameters are presented in Table 2. The upper and lower bounds of the model parameters are determined by the percentage of instability relative to the nominal model parameters in Table 2.

Table 2. The Uncertain Structural Parameters

| Uncertainty | Body Mass $m_0$ (kg) | Damping Coefficient $c_0$ (Ns/m) | Suspension Stiffness $k_0$ (N/m) |
|---|---|---|---|
| Norminal value | 1150 | 1400 | 30000 |
| Upper bound (+ 50%) | 1725 | 2100 | 45000 |
| Lower bound (- 50%) | 575 | 700 | 15000 |

### 4.2. Simulation Results in the Frequency Domain

The frequency domain simulation results of the nominal model are represented by the red star-shaped markers, while the simulation results for the model with uncertain structural parameters are depicted by the solid black lines.

***a) Varying the body mass:*** $m = 50\%m_0 \div 150\%m_0$

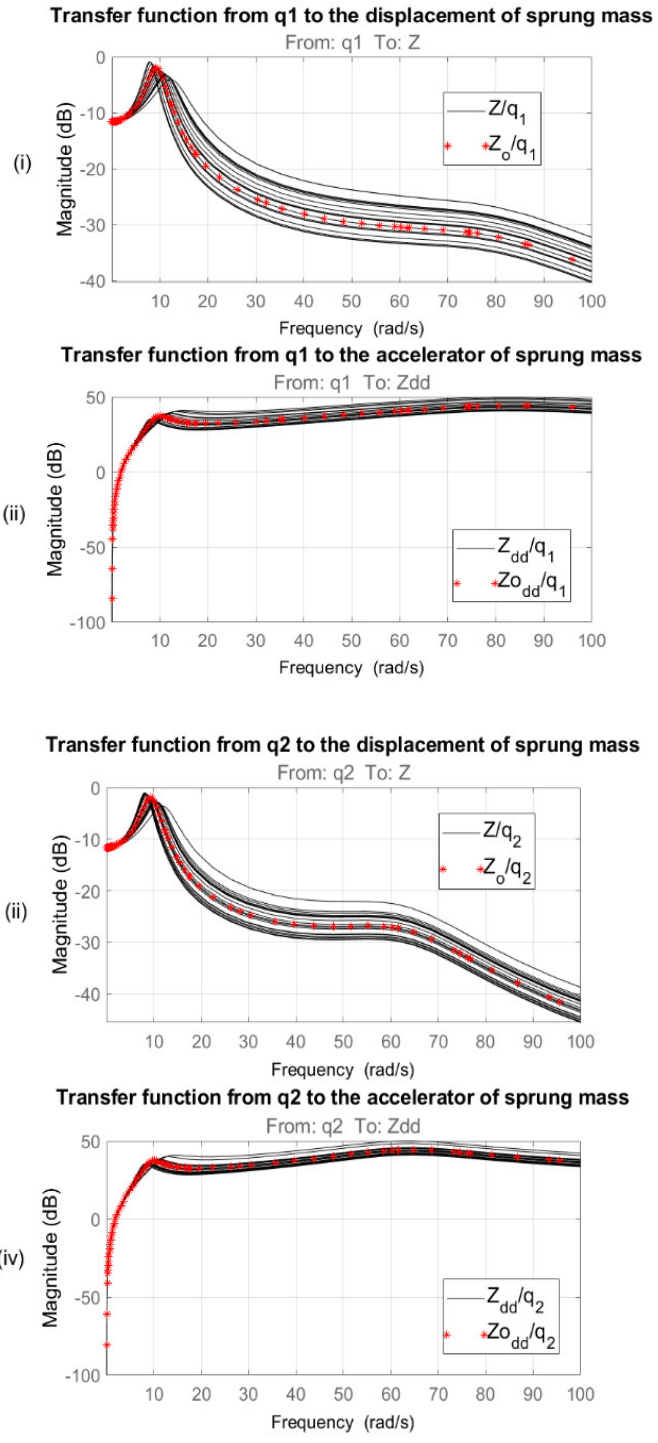

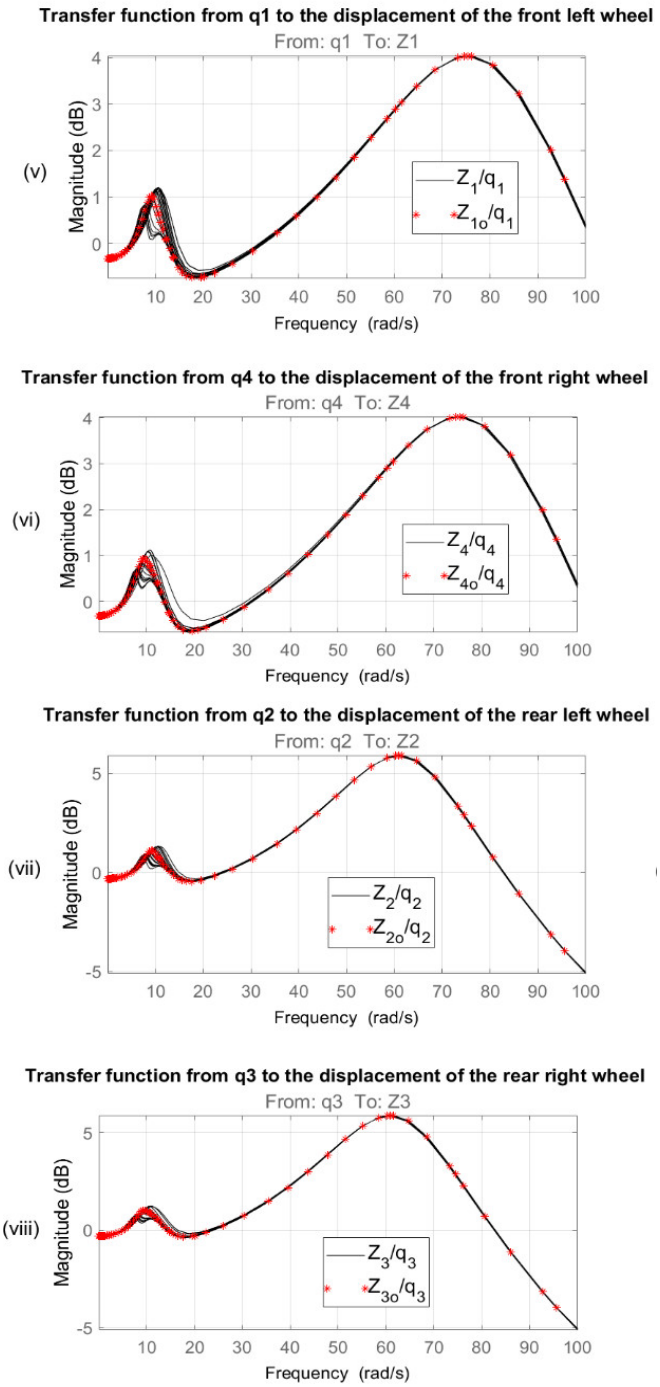


Figure 2. The graph shows the suspension system's vibrations in the frequency domain when varying m

Figures (2.i) and (2.ii) show that in the frequency range from 0 to 4 rad/s, the uncertainty has a minor effect on the vehicle body displacement. A resonance region appears between 12 and 15rad/s, and for frequencies above 15 rad/s, the transfer function for the uncertain parameters deviates by about 10 dB compared to the nominal value. Figures (2.iii) and (2.iv) indicate that in the frequency range from 0 to 4 rad/s, the uncertainty has a minor effect on the acceleration of the vehicle body displacement, and for frequencies above 15 rad/s, the transfer function for the uncertain parameters deviates by about 10 dB compared to the nominal value. In Figures (2.v), (2.vi), (2.vii), and (2.viii), when varying the vehicle body mass, the wheel displacement graph shows the largest resonance region between 5 and 25rad/s, with decreasing influence thereafter

***b) When varying the damping coefficient:*** $c = 50\%c_0 \div 150\%c_0$

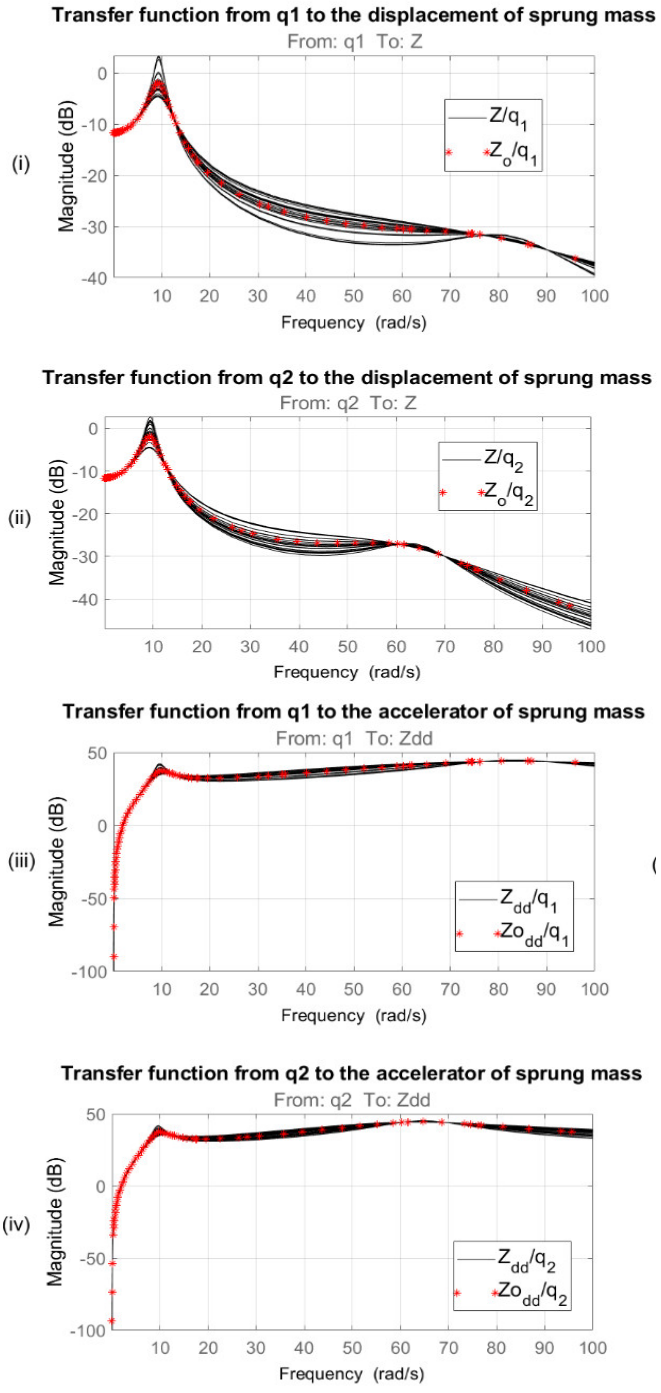

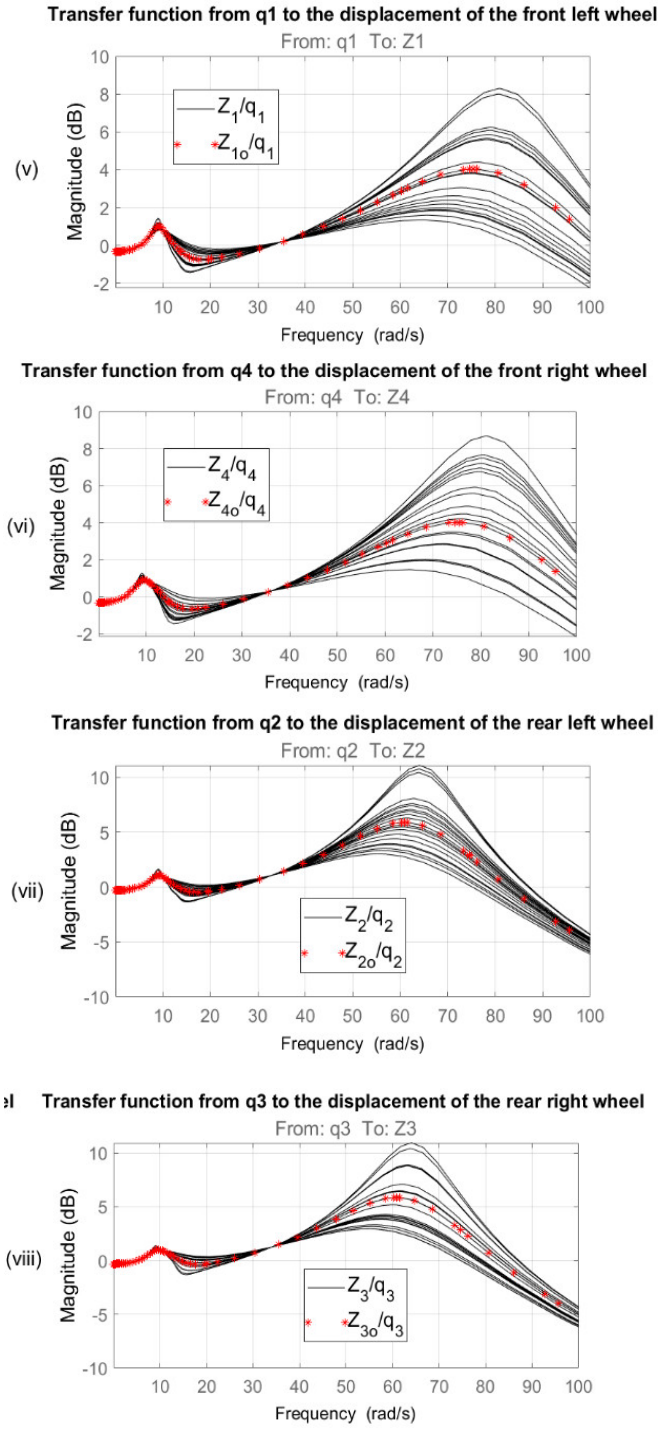


Figure 3. The graph shows the suspension system's vibrations in the frequency domain when varying the damping coefficient C

Figures (3.i) and (3.ii) show that in the frequency range from 0 to 8rad/s, the uncertainty has a minor effect on the vehicle body displacement. A resonance region appears between 8 and 15rad/s, and for frequencies above 15rad/s, the transfer function for the uncertain parameters deviates by about 5dB compared to the nominal value. Figures (3.iii) and (3.iv) indicate that the uncertainty has only a minor effect on the acceleration of the vehicle body displacement at the two wheels. In Figures (3.v), (3.vi), (3.vii), and (3.viii), when varying the vehicle body mass, the wheel displacement graph shows the largest resonance region between 40 and 100rad/s.

***c) When varying the tire stiffness:*** $\boldsymbol{k = 50\%k_0 \div 150\%k_0}$

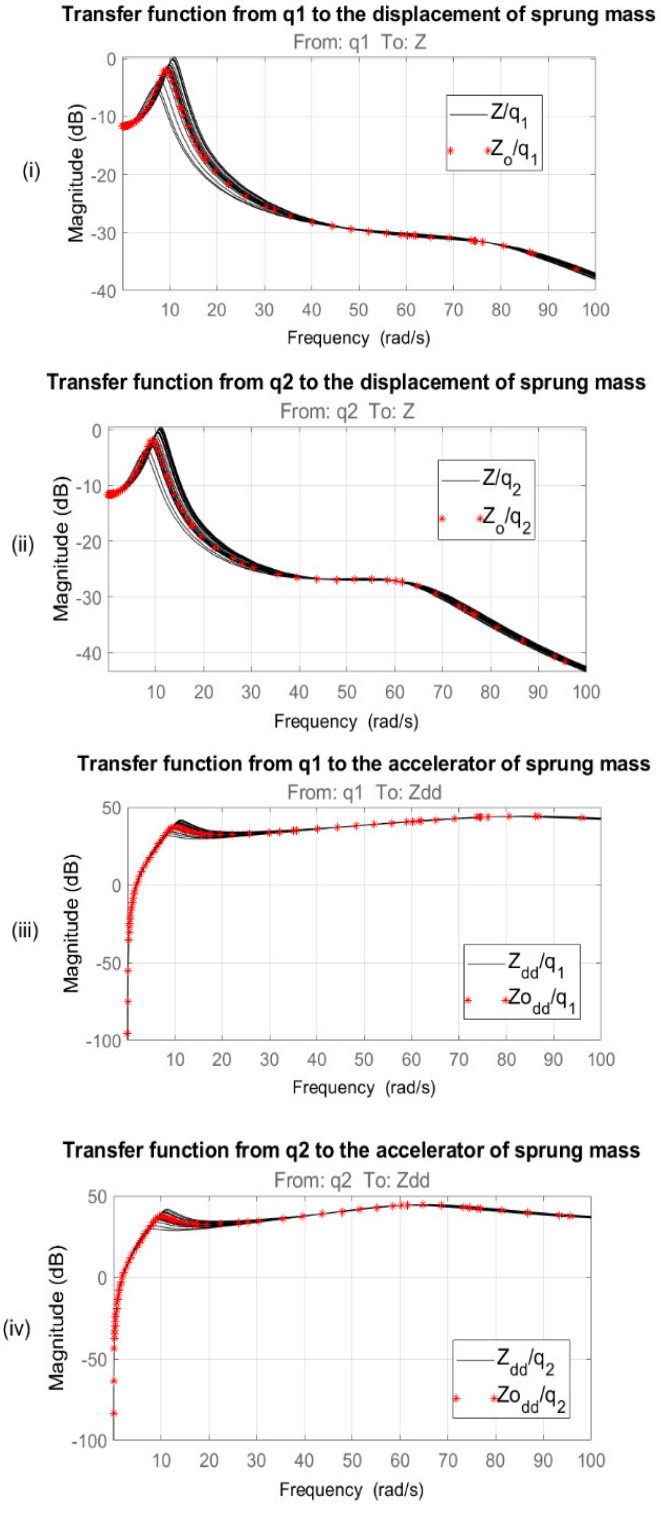

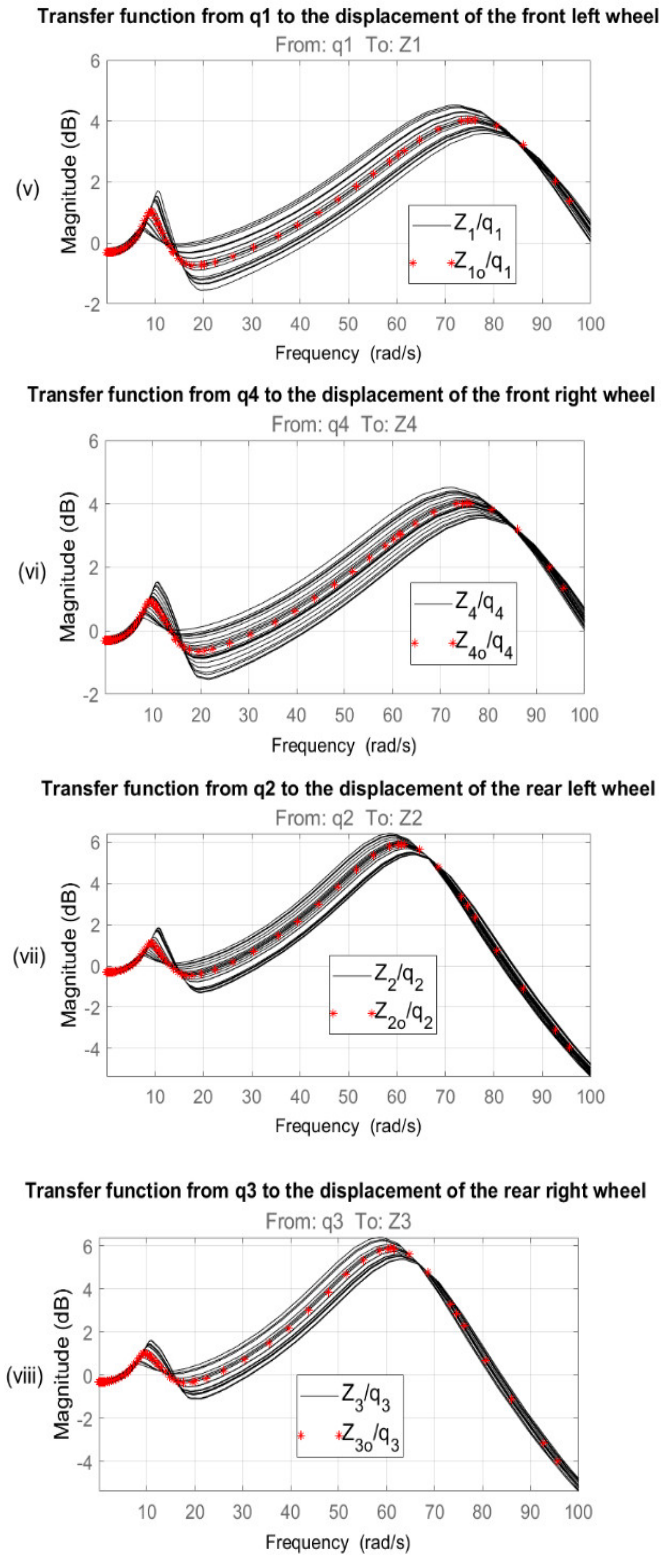


Figure 4. The graph shows the suspension system's vibrations in the frequency domain when varying the tire stiffness k

Figures (4.i) and (4.ii) show that in the frequency range from 0 to 5rad/s, the uncertainty has a minor effect on the vehicle body displacement. A resonance region appears between 10 and 25rad/s, and for frequencies above 25rad/s, the transfer function for the uncertain parameters changes insignificantly. Figures (4.iii) and (4.iv) indicate that the uncertainty has only a minor effect on the acceleration of the vehicle body displacement at the two wheels in the range of 10 to 20rad/s. In Figures (4.v), (4.vi), (4.vii), and (4.viii), when varying the vehicle body mass, the wheel displacement graph shows the largest resonance region between 40 and 100rad/s.

### 4.3. Simulation Results in the Time Domain

The time domain simulation results of the model are presented through the Root Mean Square (RMS) value and the maximum absolute value MAX(ABS) of the signals. The values for the vehicle body mass, damping coefficient and suspension stiffness; are varied from 50% to 150% of the nominal values as shown in Table 2. In the time domain survey results, the red dashed lines represent the maximum absolute values MAX(ABS) of the indicators, while the RMS value simulation results are depicted by the solid blue lines.

***a) Varying the body mass:*** $\boldsymbol{m = 50\%m_0 \div 150\%m_0}$

In Figures (5.i), (5.iii), and (5.iv), when varying the vehicle body mass, both RMS and MAX(ABS) values of the indicators increase significantly. For the vehicle body displacement acceleration indicator in Figure (5.ii), both RMS and MAX(ABS) values remain almost unchanged.

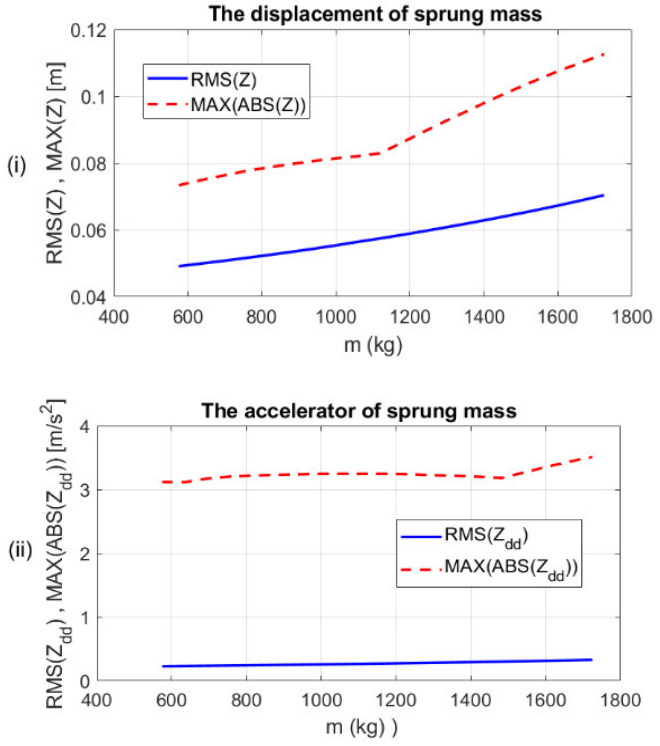

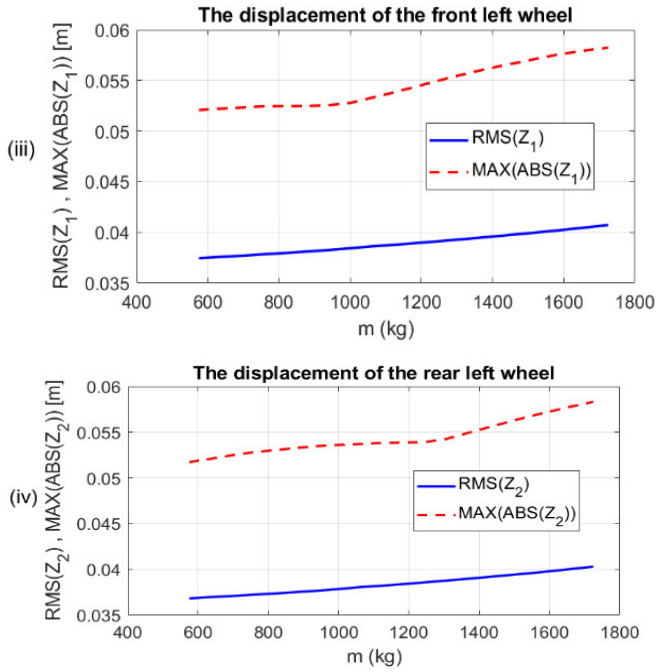


Figure 5. The graph shows the suspension system's vibrations in the time domain when varying body mass m

***b) When varying the damping coefficient:*** $c = 50\%c_0 \div 150\%c_0$

In Figures (6.i) and (6.ii), when increasing the damping coefficient c, the MAX(ABS) values for both body displacement and body acceleration decrease significantly, while the RMS values remain almost unchanged. For the wheel displacement indicators in Figures (6.iii) and (6.iv), both RMS and MAX(ABS) values decrease slightly, but not significantly.

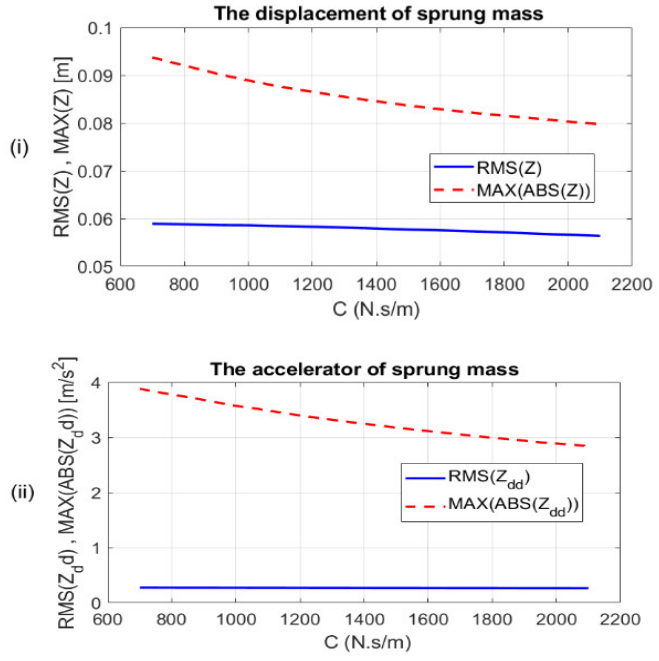


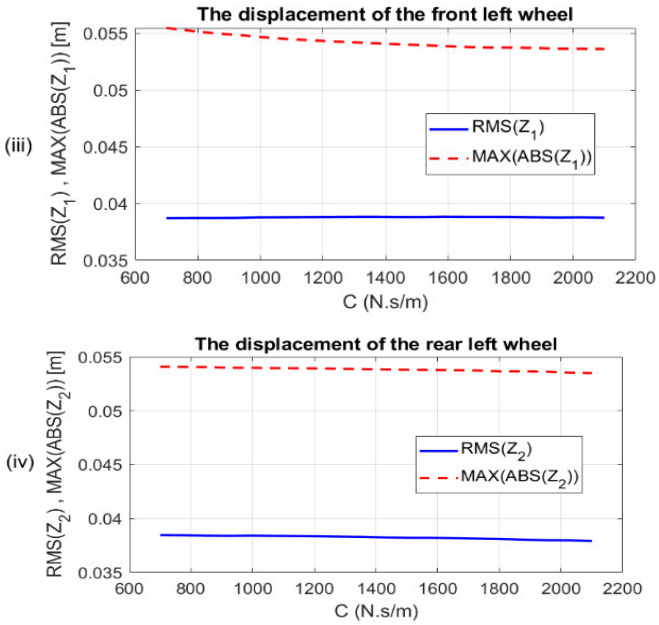


Figure 6. The graph shows the suspension system's vibrations in the time domain when varying the damping coefficient c

***c) When varying the tire stiffnes:*** $k = 50\%k_0 \div 150\%k_0$

In Figure (7.i), as the tire stiffness k increases, the MAX(ABS) value of the vehicle body displacement decreases significantly when k changes from 15,000 to 30,000 N/m; beyond 30,000 N/m, it remains almost unchanged, and the RMS value of the displacement decreases sharply. For the indicators in Figures (7.ii), (7.iii), and (7.iv), the MAX(ABS) value in Figure (7.ii) increases significantly, while in Figures (7.iii) and (7.iv), it changes only slightly. The RMS values in all three cases decrease only slightly.

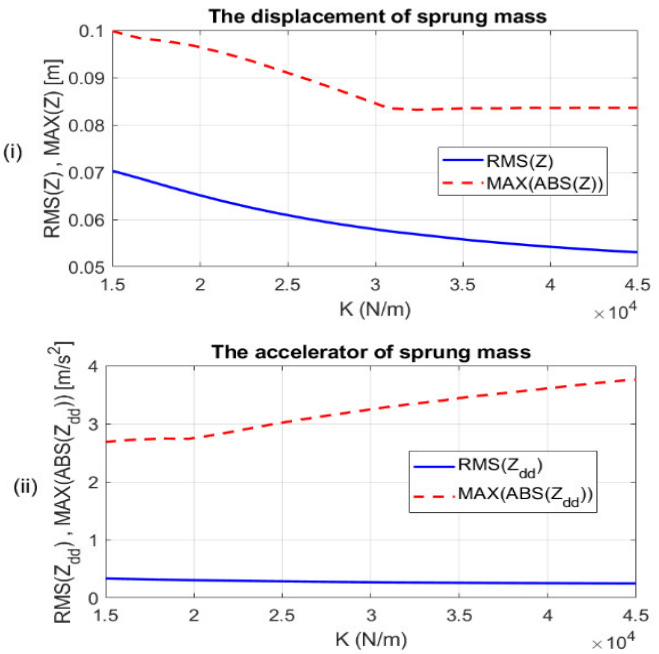

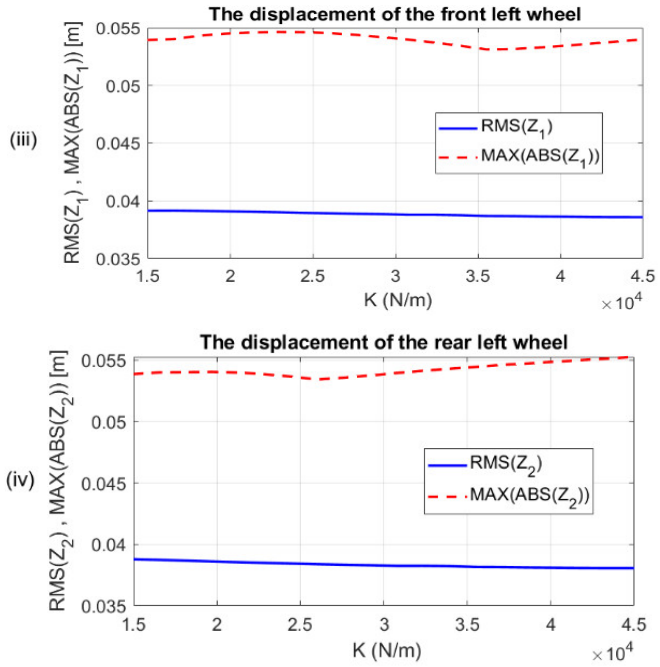


Figure 7. The graph shows the suspension system's vibrations in the time domain when varying the tire stiffness k

The simulation results in both the time and frequency domains demonstrate the characteristics of the full vehicle model when considering the uncertainty of structural parameters. The research findings indicate that the uncertainty of structural parameters significantly affects the performance and characteristics of the suspension system in passenger cars. According to the research results, the values for body displacement, acceleration, and roll angles change significantly when the nominal values of the uncertain parameters are altered.

## 5. CONCLUSION

In this paper, the authors focus on developing a 7-degree-of-freedom vehicle dynamics model to assess the system's comprehensiveness, establish dynamic equations, and transition to state-space representation. The study examines how parameters such as vehicle body mass, damping coefficient, and suspension stiffness affect vehicle vibrations and stability when varying these parameters within a range of 50 - 150% of their nominal values. The simulation results in both time and frequency domains demonstrate the model's characteristics when considering the uncertainty of structural parameters. The research shows that the uncertainty of these parameters has a significant impact on the performance and characteristics of passive suspension systems in vehicles. Based on these findings, the authors plan to further investigate additional uncertain parameters that may affect vehicle vibrations and develop a comprehensive control method for active suspension system to mitigate the effects of parameter uncertainty, leveraging the evaluation results and simulation equations from this study.

## REFERENCES

[1]. Semiha Turkay, Huseyin Akcay, "Aspects of achievable performance for quarter-car active suspensions," *IFAC Proceedings Volumes*, 40, 10, 207-212, 2007.

[2]. Kothari Priyank, Mulla Muzamil, Bathe Nachiket, *Modeling of Active and Passive suspension system for half car model*. University of Michigan, 2024. DOI: 10.13140/RG.2.2.35723.30247.

[3]. Semiha Turkey, Huseyin Akcay, "A study of random vibration characteristics of the quarter-car model," *Journal of Sound and Vibration*, 282, 1-2, 111-124, 2005. DOI: 10.1016/j.jsv.2004.02.049.

[4]. W. Gao, N. Zhang, J. C. Ji, H. P. Du, "Dynamic analysis of vehicles with uncertainty," in *Proceedings of the Institution of Mechanical Engineers, Part D: Journal of Automobile Engineering*, 222, 5, 657-664, 2008. DOI: 10.1243/09544070JAUTO740.

[5]. Georgiou G., Verros G., Natsiavas S., "Multiobjective optimization of quarter-car models with a passive or semi-active suspension system," *Vehicle System Dynamics*, 45, 1, 77-92, 2007. DOI: 10.1080/00423110600812925.

[6]. Kim H. J., Yang H. S., Park Y. P., "Improving the vehicle performance with active suspension using road-sensing algorithm," *Computers & Structures*, 80, 18-19, 1569-1577, 2002. DOI: 10.1016/S0045-7949(02)00110-4.

[7]. Papalukopoulos C., Natsiavas S., "Nonlinear biodynamics of passengers coupled with quarter car models," *Journal of Sound and Vibration*, 304, 1-2, 50-71, 2007. DOI: 10.1016/j.jsv.2007.01.042.

[8]. Abougarair Ahmed, "Design and Simulation Optimal Controller For Quarter Car Active Suspension System," in *1st Conference of Industrial Technology* (CIT2017), 2019.

[9]. Werner Schiehlen, Igor Iroz, "Dynamical Analysis of Multibody Systems with Design Uncertainties," *Procedia IUTAM*, 13, 151-159, 2015.

[10]. Yoshimura T., Nakaminami K., Kurimoto M., Hino J., "Active suspension of passenger cars using linear and fuzzy-logic controls," Control Engineering Practice, 7, 1, 41-47, 1999. DOI: 10.1016/S0967-0661(98)00145-2.

[11]. Thompson A. G., Davis B. R., "Computation of the rms state variables and control forces in a half-car model with preview active suspension using spectral decomposition methods," *Journal of Sound and Vibration*, 285, 3, 571-583, 2005. DOI: 10.1016/j.jsv.2004.08.017.

[12]. Marzbanrad J., Ahmadi G., Zohoor H., Hojjat Y., "Stochastic optimal preview control of a vehicle suspension," *Journal of Sound and Vibration*, 275, 3-5, 973-990, 2004. DOI: 10.1016/S0022-460X(03)00812-5.

[13]. Rosheila Darus, Yahaya Md. Sam, "Modeling and control of active suspension for a full car model," in *5th International Colloquium on Signal Processing & Its Applications*, 13-18, 2009.

[14]. Claudio Gattia, Marcelo T. Piovan, "Dynamic analysis of models for suspension systems of ground vehicles with uncertain parameters," *MECOM 2012, X Argentine Congress of Computational Mechanics*, XXXI, 2745-2755, 2012.

[15]. Vũ Hải Quân, Lê Hữu Chúc, "Mô hình hóa và điều khiển hệ thống treo tích cực cho mô hình toàn xe," *Tạp chí Khoa học và Công nghệ, Trường Đại học Công nghiệp Hà Nội*, 56, 2, 2020.

[16]. Yi-jie Chen, Qiang-shun Lei, Xu Zhang, Guan-hui Zheng, Ya-feng Zhang, "Suspension System Dynamics Modeling and Simulation Analysis," *DEStech Transactions on Engineering and Technology Research,* 2017. DOI: 10.12783/dtetr/icamm2016/7397.

[17]. Do Trong Tu, Vu Van Tan, Olivier Seaname, "Parameter uncertainty analysis for electro-hydraulic servo-valve actuator of active suspension system on trucks," *TNU Journal of Science and Technology,* 160-169, 2023. DOI: 10.34238/tnu-jst.8792.

[18]. P. Gaspar, Z. Szabo, J. Bokor, "Active Suspension in Integrated Vehicle Control," *Switched Systems*, 2009.

[19]. Dang Viet Ha, Vu Van Tan, Vu Thanh Niem, Olivier Sename, "Evaluation of Dynamic Load Reduction for a Tractor Semi-Trailer Using the Air Suspension System at all Axles of the Semi-Trailer," *Actuators,* 11, 1, 2023. DOI:10.3390/act11010012.

[20]. J. Zhu, D. Zhao, S. Liu, Z. Zhang, G. Liu, J. Chang, "Integrated Control of Spray System and Active Suspension Systems Based on Model-Assisted Active Disturbance Rejection Control Algorithm," *Mathematics,* 10, 18, 2022. DOI: 10.3390/math10183391.

[21]. Truong Manh Hung, "Optimal selection for an air suspension system on buses through a unique high-level parameter in genetic algorithms," *Heliyon*, 8, 3, Article e09059, 2022. DOI: 10.1016/j.heliyon.2022.e09059

[22]. Vu Van Tan, "Two-Layer Parallel Fuzzy Logic Controller Design for Semiactive Suspension System with a Full Car Model", *Shock and Vibration*, Article ID 7020462, 2023. https://doi.org/10.1155/2023/7020462

**THÔNG TIN TÁC GIẢ**

**Nguyễn Ngọc Trâm[1], Kiều Đức Thịnh[1], Vũ Văn Tấn[2], Olivier Sename[3]**

[1]Khoa Cơ khí, Trường Đại học Thủy lợi

[2]Khoa Cơ Khí, Trường Đại học Giao thông Vận tải

[3]Trường Đại học Grenoble Alpes, Cộng hòa Pháp